JCI The Journal of Clinical Investigation

Circulating T follicular regulatory and helper cells have memory-like properties

Peter T. Sage, … , Ulrich H. von Andrian, Arlene H. Sharpe

J Clin Invest. 2014;124(12):5191-5204. https://doi.org/10.1172/JCI76861.

Research Article **Immunology**

Follicular Tregs (Tfr cells) inhibit antibody production, whereas follicular Th cells (Tfh cells) stimulate it. Tfr cells are found in blood; however, relatively little is known about the developmental signals for these cells or their functions. Here we demonstrated that circulating Tfr and Tfh cells share properties of memory cells and are distinct from effector Tfr and Tfh cells found within lymph nodes (LNs). Circulating memory-like Tfh cells were potently reactivated by DCs, homed to germinal centers, and produced more cytokines than did effector LN Tfh cells. Circulating memory-like Tfr cells persisted for long periods of time in vivo and homed to germinal centers after reactivation. Effector LN Tfr cells suppressed Tfh cell activation and production of cytokines, including IL-21, and inhibited class switch recombination and B cell activation. The suppressive function of this population was not dependent on specific antigen. Similar to LN effector Tfr cells, circulating Tfr cells also suppressed B and Tfh cells, but with a much lower capacity. Our data indicate that circulating memory-like Tfr cells are less suppressive than LN Tfr cells and circulating memory-like Tfh cells are more potent than LN effector Tfh cells; therefore, these circulating populations can provide rapid and robust systemic B cell help during secondary antigen exposure.

Circulating T follicular regulatory and helper cells have memory-like properties

Peter T. Sage,[1,2] David Alvarez,[1] Jernej Godec,[1,2] Ulrich H. von Andrian,[1] and Arlene H. Sharpe[1,2,3]

[1]Department of Microbiology and Immunobiology, Harvard Medical School, Boston, Massachusetts, USA. [2]Evergrande Center for Immunologic Diseases, Harvard Medical School and Brigham and Women's Hospital, Boston, Massachusetts, USA. [3]Department of Pathology, Brigham and Women's Hospital, Boston, Massachusetts, USA.

Follicular Tregs (Tfr cells) inhibit antibody production, whereas follicular Th cells (Tfh cells) stimulate it. Tfr cells are found in blood; however, relatively little is known about the developmental signals for these cells or their functions. Here we demonstrated that circulating Tfr and Tfh cells share properties of memory cells and are distinct from effector Tfr and Tfh cells found within lymph nodes (LNs). Circulating memory-like Tfh cells were potently reactivated by DCs, homed to germinal centers, and produced more cytokines than did effector LN Tfh cells. Circulating memory-like Tfr cells persisted for long periods of time in vivo and homed to germinal centers after reactivation. Effector LN Tfr cells suppressed Tfh cell activation and production of cytokines, including IL-21, and inhibited class switch recombination and B cell activation. The suppressive function of this population was not dependent on specific antigen. Similar to LN effector Tfr cells, circulating Tfr cells also suppressed B and Tfh cells, but with a much lower capacity. Our data indicate that circulating memory-like Tfr cells are less suppressive than LN Tfr cells and circulating memory-like Tfh cells are more potent than LN effector Tfh cells; therefore, these circulating populations can provide rapid and robust systemic B cell help during secondary antigen exposure.

Introduction

Follicular Th cells (Tfh cells), a subset of $CD4^+$ T cells, stimulate and maintain the germinal center (GC) reaction, enabling B cells to produce high-affinity antibodies. Tfh cells are defined by CXCR5, which directs them to the B cell zone via gradients of the chemokine CXCL13 (1, 2). Tfh cells express the transcription factor BCL6, which facilitates CXCR5 expression and stimulates IL-21 production, helping B cells to undergo affinity maturation and produce antibody (3–5). Tfh cells also can produce other cytokines, including IFN-γ, IL-17, and IL-4, which may help with selection of antibody isotypes during class switch recombination.

Follicular Tregs (Tfr cells) are a newly defined population of $CXCR5^+$ $CD4^+$ T cells. Like Tfh cells, Tfr cells express high levels of CXCR5, ICOS, and PD-1 (6–9). However, Tfr cells are thought to originate in the periphery from thymic-derived Treg (tTreg) precursors, in contrast to Tfh cells, which develop from naive $FOXP3^-$ T cells (7, 9). Importantly, Tfr and Tfh cells have opposing roles in regulating humoral immunity: whereas Tfr cells potently suppress humoral immune responses, Tfh cells stimulate them (6–9). The mechanisms by which Tfr cells suppress the GC reaction are still unclear. It is not known whether Tfr cells suppress Tfh cells, GC B cells, or both. Moreover, whether specific antigen is required for Tfr suppression is also not known. Understanding how Tfr cells inhibit humoral immunity has the potential to enable improved vaccination strategies.

Tfr and Tfh cells are present not only in lymph nodes (LNs), but also in the circulation (9). Circulating Tfh cells from humans can provide help to B cells in vitro (10, 11), and circulating Tfh cells from mice can stimulate B cells in vivo (9). A subset of human blood Tfh cells has been postulated to represent memory cells (1, 10, 12). This putative memory Tfh cell subset expresses CXCR5 comparably to LN Tfh cells, but expresses less PD-1 and ICOS. However, bona fide Tfh cell memory has not been demonstrated in vivo. It is possible that circulating Tfh cells may give rise to memory Tfh cells (9, 13, 14). Likewise, circulating Tfr cells also may have memory potential.

Elucidating the relationships between LN Tfr and Tfh cells and circulating Tfr and Tfh cells may provide insights into their memory cell development and function (2). Although LN Tfr and Tfh cells depend on CD28, ICOS, and B cells for development, the specific cues for blood Tfr and Tfh cell development and maintenance are not yet clear (9). It has been suggested that blood Tfh cells do not require the GC reaction for differentiation, but whether this is true for Tfr cells is unknown (15). Circulating Tfh cells in humans appear to differ from LN Tfh cells, as assessed by microarray analysis; however, these differences may be due to decreased activation in the blood or contaminating Tfr cells (12).

The most straightforward explanation for Tfr and Tfh cells in the circulation is that some Tfr and Tfh cells in the GC leave the LN. If this hypothesis were true, then circulating Tfr and Tfh cells would require LN Tfr and Tfh cells for their development. In support of this hypothesis, Tfr and Tfh cells are almost completely missing from the LNs and blood of CD28- and ICOS-deficient mice (9, 16, 17). However, PD-1–deficient mice have increased Tfh cells in the blood, but not in the LN (9). In addition, LN Tfr and Tfh cells develop with kinetics similar to those of blood Tfh and Tfr cells (9). Moreover, recent tracking experiments suggest that GC Tfh cells are unable to gain access to the circulation (18). These findings suggest that circulating and LN Tfr and Tfh cells may develop independently.

Conflict of interest: The authors have declared that no conflict of interest exists.
Submitted: April 30, 2014; **Accepted:** September 25, 2014.
Reference information: *J Clin Invest*. 2014;124(12):5191–5204. doi:10.1172/JCI76861.

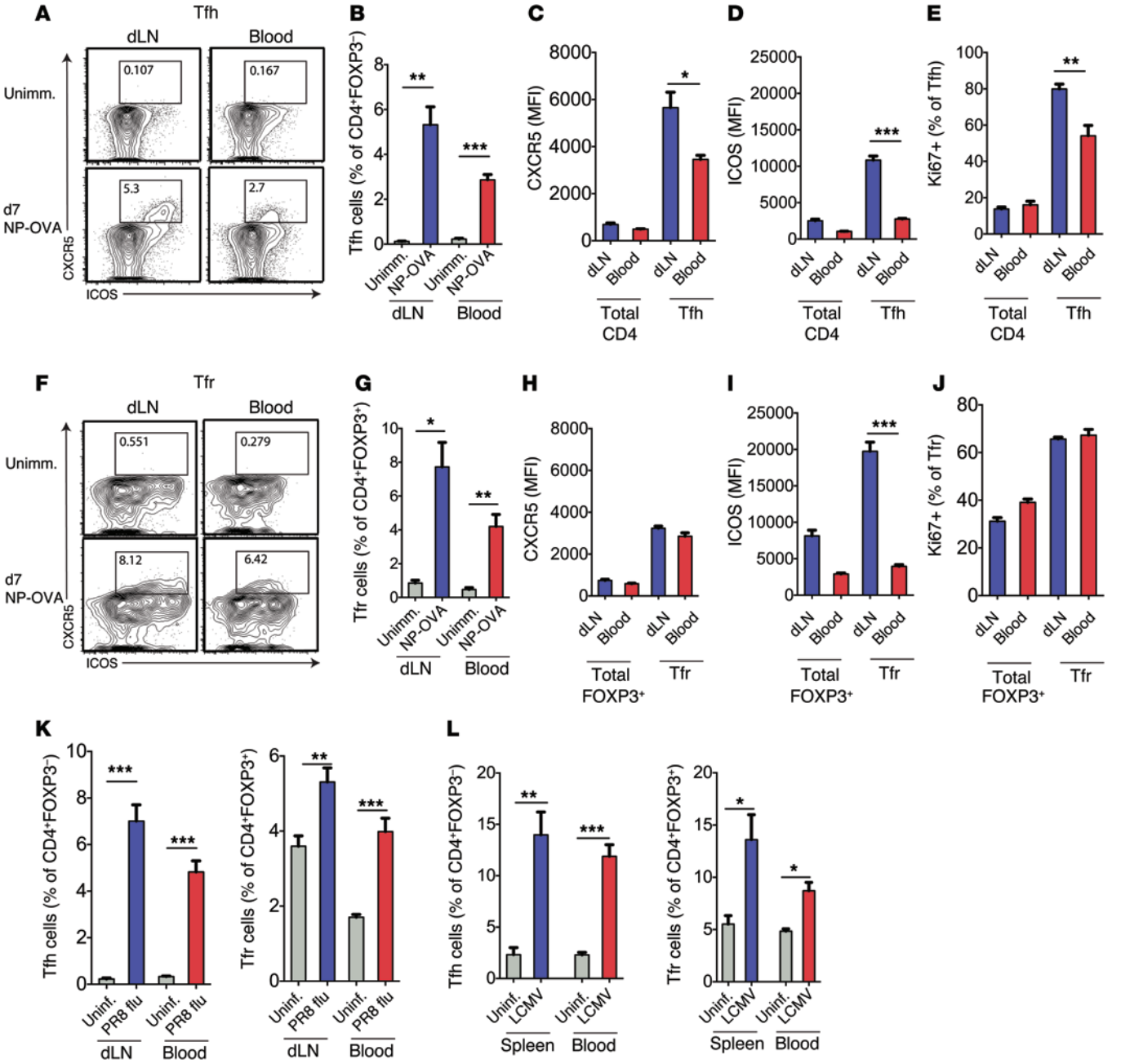

Figure 1. Phenotype of circulating Tfh and Tfr cells. (**A**–**J**) WT mice were immunized s.c. with NP-OVA, and dLN and blood were analyzed for Tfh (**A**–**E**) and Tfr (**F**–**J**) cells on day 7. Unimm., unimmunized control. (**A** and **F**) Plots pregated on $CD4^+FOXP3^-CD19^-$ (**A**) or $CD4^+FOXP3^+CD19^-$ (**F**); number indicates percent in gate. (**B** and **G**) Quantification of cell subpopulations from plots. (**C**–**E** and **H**–**J**) Quantification of CXCR5 (**C** and **H**), ICOS (**D** and **I**), and Ki67 (**E** and **J**) expression. Total $CD4^+CD19^-$ (Total CD4; **C**–**E**) and total $CD4^+FOXP3^+CD19^-$ cells (Total $FOXP3^+$; **H**–**J**), are included as controls. (**K**) Tfh and Tfr cells in dLN and blood on d10 after PR8 influenza (PR8 Flu) infection. (**L**) Tfh and Tfr cells in spleen and blood on d7 after LCMV CL13 infection. Uninf., uninfected control. Data are mean ± SEM with 5 mice per group and representative of ≥3 independent experiments. $^*P < 0.05$, $^{**}P < 0.01$, $^{***}P < 0.001$, unpaired Student's *t* test.

Here, we demonstrated that blood Tfr and Tfh cells are distinct and specialized cellular subsets that have properties of memory cells. Circulating memory-like Tfr and Tfh populations differed from "effector" Tfr and Tfh cells in several ways. Circulating memory-like Tfr and Tfh cells could circulate throughout the body patrolling for antigen for long periods of time. Upon homing to LNs, circulating memory-like Tfh cells required repriming by DCs to become functional and produced more cytokines than LN effector Tfh cells. Compared with LN Tfr cells, circulating memory-like Tfr cells exhibited decreased suppressive capacity. However, LN and circulating Tfr cells similarly suppressed Tfh cell activation as well as B cell activation and class switch recombination. Since circulating memory-like Tfh cells were more potently activated and circulating memory-like Tfr cells were less suppressive, we conclude that the blood $CD4^+CXCR5^+$ population as a whole is poised to form a quick memory-like response wherever reexposure to antigen may occur.

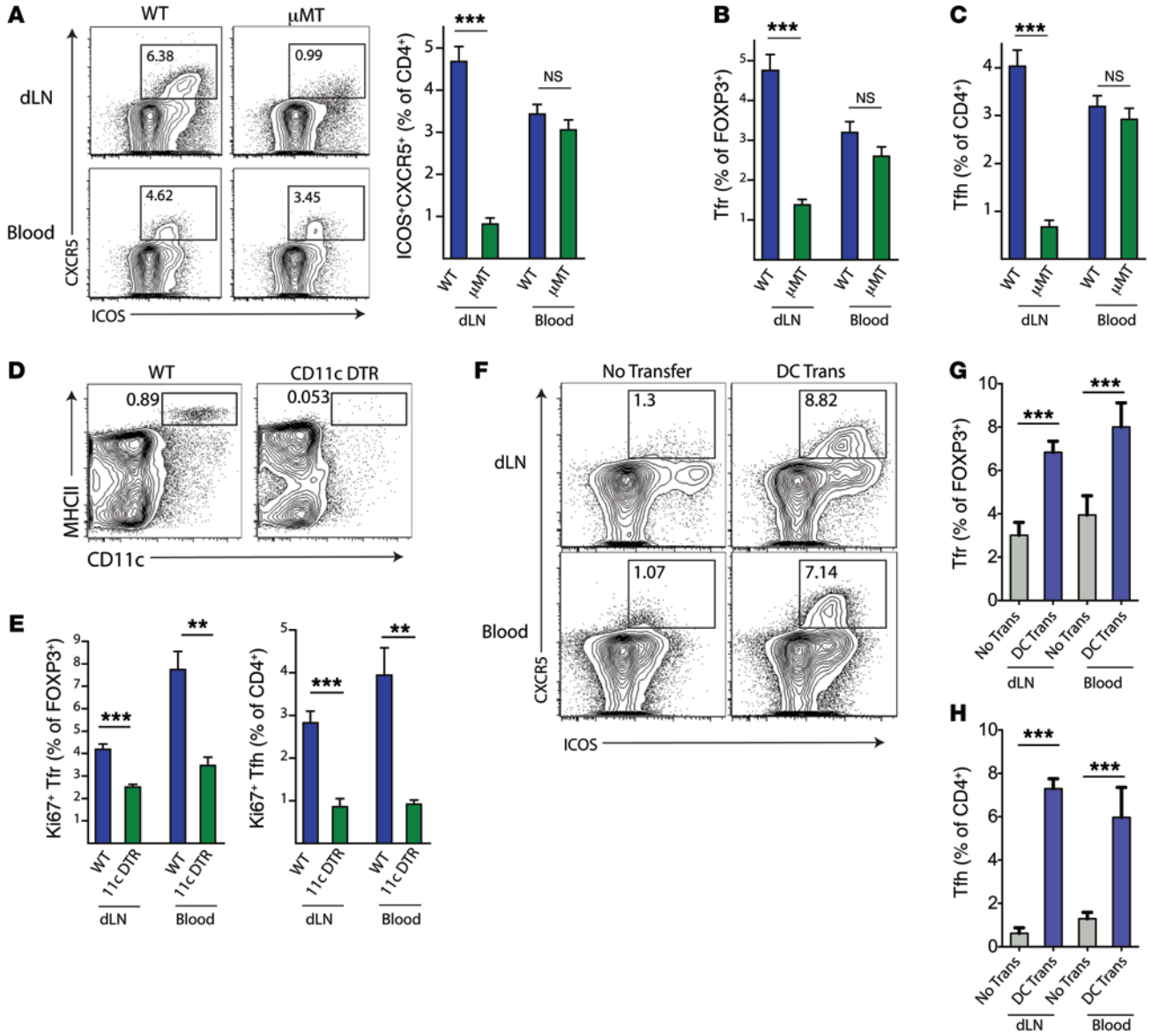

Figure 2. Circulating Tfr cells require DCs for development. (**A**–**C**) B cells are not required for circulating Tfr and Tfh cell differentiation. WT or μMT mice were immunized s.c. with NP-OVA; 7 days later, $CD4^+ICOS^+CXCR5^+$ cells were analyzed. (**A**) Representative plots (pregated on $CD4^+CD19^-$; number indicates percent in gate) and quantification. (**B**) Tfr ($CD4^+ICOS^+CXCR5^+FOXP3^+CD19^-$) and (**C**) Tfh ($CD4^+ICOS^+CXCR5^+FOXP3^-CD19^-$) cells after immunization. (**D** and **E**) WT or CD11c-DTR BM chimeras were immunized s.c. with NP-OVA, and DT was administered on d0, d2, d4, and d6. (**D**) dLN analysis of $CD11c^+MHCII^+$ DCs; number indicates percent of cells in gate. (**E**) Quantification of $Ki67^+$ Tfr cells (percentage of total $FOXP3^+$ cells) and $Ki67^+$ Tfh cells (percentage of total $CD4^+$ T cells) in dLN and blood. (**F**–**H**) DC transfer experiments. WT BMDCs were pulsed with NP-OVA and transferred s.c. to WT mice (DC Trans); 7 days later, dLNs and blood were analyzed. WT mice that received no transfer were included as controls. (**F**) Representative plots (pregated on $CD4^+CD19^-$; number indicates percent of cells in gate). (**G** and **H**) Quantification of dLN and blood Tfr (**G**) and Tfh (**H**) cells. Data are mean ± SEM with 5 mice per group and representative of ≥3 independent experiments. $^{**}P < 0.01$, $^{***}P < 0.001$, unpaired Student's *t* test.

Results

Circulating Tfr cells expand after protein immunization or viral infection. To determine whether blood and LN Tfr cells have phenotypic differences, we compared the expression of CXCR5 and other cell surface markers. We analyzed CXCR5 and ICOS expression on circulating and LN cells after immunization with 4-hydroxy-3-nitrophenylacetyl hapten–conjugated OVA (NP-OVA) in CFA, which causes differentiation of Tfr and Tfh cells (9). Tfh cells ($CD4^+ICOS^+CXCR5^+FOXP3^-CD19^-$) expanded in the draining LNs (dLNs) and blood of immunized mice (Figure 1, A and B). Compared with dLN Tfh cells, blood Tfh cells had lower — albeit still substantial — expression of CXCR5, ICOS, and Ki67 (Figure 1, C–E). Tfr cells ($CD4^+ICOS^+CXCR5^+FOXP3^+CD19^-$) differentiated significantly in both dLNs and blood (Figure 1, F and G). Compared with dLN Tfr cells, blood Tfr cells expressed similar levels of CXCR5, but lower ICOS (Figure 1, H and I). Ki67 staining revealed similar proportions of dLN and blood Tfr cells in cell cycle (Figure 1J). Tfh and Tfr cell numbers in the blood of mice infected with influenza or with lymphocytic choriomeningitis virus (LCMV) also expanded, and these cells expressed ICOS similar to levels in NP-

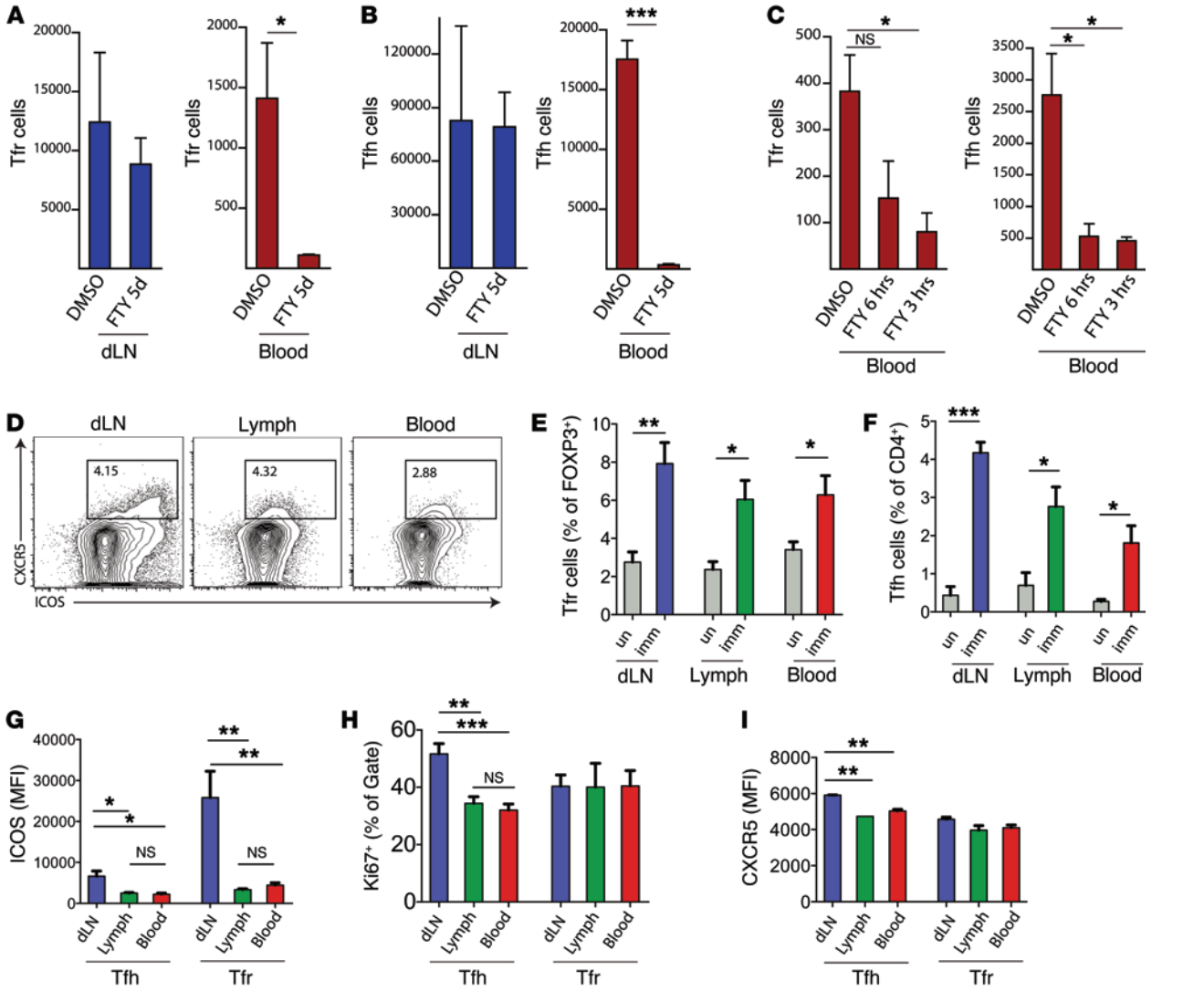

Figure 3. Circulating Tfr cells have a distinct phenotype when exiting the LN. (**A** and **B**) Tfr cells (**A**) or Tfh cells (**B**) in the dLN and per ml blood after FTY720 treatment for 5 days (d2, d4, and d6 after immunization, followed by analysis on d7). (**C**) Tfr and Tfh cells (per ml blood) after FTY720 treatment during the last 3 or 6 hours of a 7-day immunization. (**D**) Representative plots of total $CD4^+ICOS^+CXCR5^+$ cells from the dLN, efferent lymph (Lymph), and blood of immunized mice. Plots are pregated on $CD4^+CD19^-$; number indicates percent of cells in gate. (**E** and **F**) Percentage of Tfr (**E**) or Tfh (**F**) cells in the dLN, efferent lymph, and blood of WT mice immunized (imm) or not (un) 7 days previously. (**G**–**I**) ICOS (**G**), Ki67 (**H**), and CXCR5 (**I**) expression on dLN, lymph, and blood Tfr and Tfh cells from experiments as in **D**. Data are mean ± SEM with 5 mice per group and representative of ≥3 independent experiments (**A**–**C**) or with mice from 5 replicate surgeries (**D**–**I**). $^*P < 0.05$, $^{**}P < 0.01$, $^{***}P < 0.001$, unpaired Student's *t* test (**A**, **B**, **E**, and **F**) or 1-way ANOVA with Tukey post-test (**C**, **G**, **H**, and **I**).

OVA–induced circulating Tfh and Tfr cells (Figure 1, K and L, and Supplemental Figure 1; supplemental material available online with this article; doi:10.1172/JCI76861DS1). However, in these viral infections, Tfh cells outnumbered Tfr cells to a greater extent than with protein immunization (data not shown).

Differentiation of circulating Tfr cells requires priming by DCs. LN Tfh cells depend on DCs for initial differentiation (19) and on B cells for maintenance (20–22). LN Tfr cells also depend on B cells for their differentiation and maintenance (6). However, B cells are not essential for development of circulating Tfh cells (15), which led us to investigate whether B cells are required for circulating Tfr cells. We immunized WT and μMT mice (which lack B cells) and compared dLN and circulating Tfr cells. As expected, Tfr and Tfh cells in the dLN were attenuated in μMT mice (Figure 2, A–C) (21). In contrast, Tfr and Tfh cells within the blood of WT and μMT mice were equivalent, which suggests that blood and LN Tfr cells require distinct cues for development, unlike LN Tfr cells.

To determine whether DCs are necessary for the generation of circulating Tfr and Tfh cells, we used BM chimeric mice (CD11c-DTR strain) to deplete DCs. Diphtheria toxin (DT) administration resulted in depletion of most DCs from CD11c-DTR mice, which consequently led to lower percentages of activated (i.e., $Ki67^+$) Tfr cells in dLNs and blood (Figure 2, D and E). These observations suggest that DCs are important for dLN and blood Tfr cell differentiation. Depletion of DCs also reduced $Ki67^+$ Tfh cell numbers (Figure 2E).

We next investigated whether antigen presentation by DCs was sufficient for Tfr cell development. We pulsed LPS-activated BM-derived DCs (BMDCs) with NP-OVA, transferred these cells

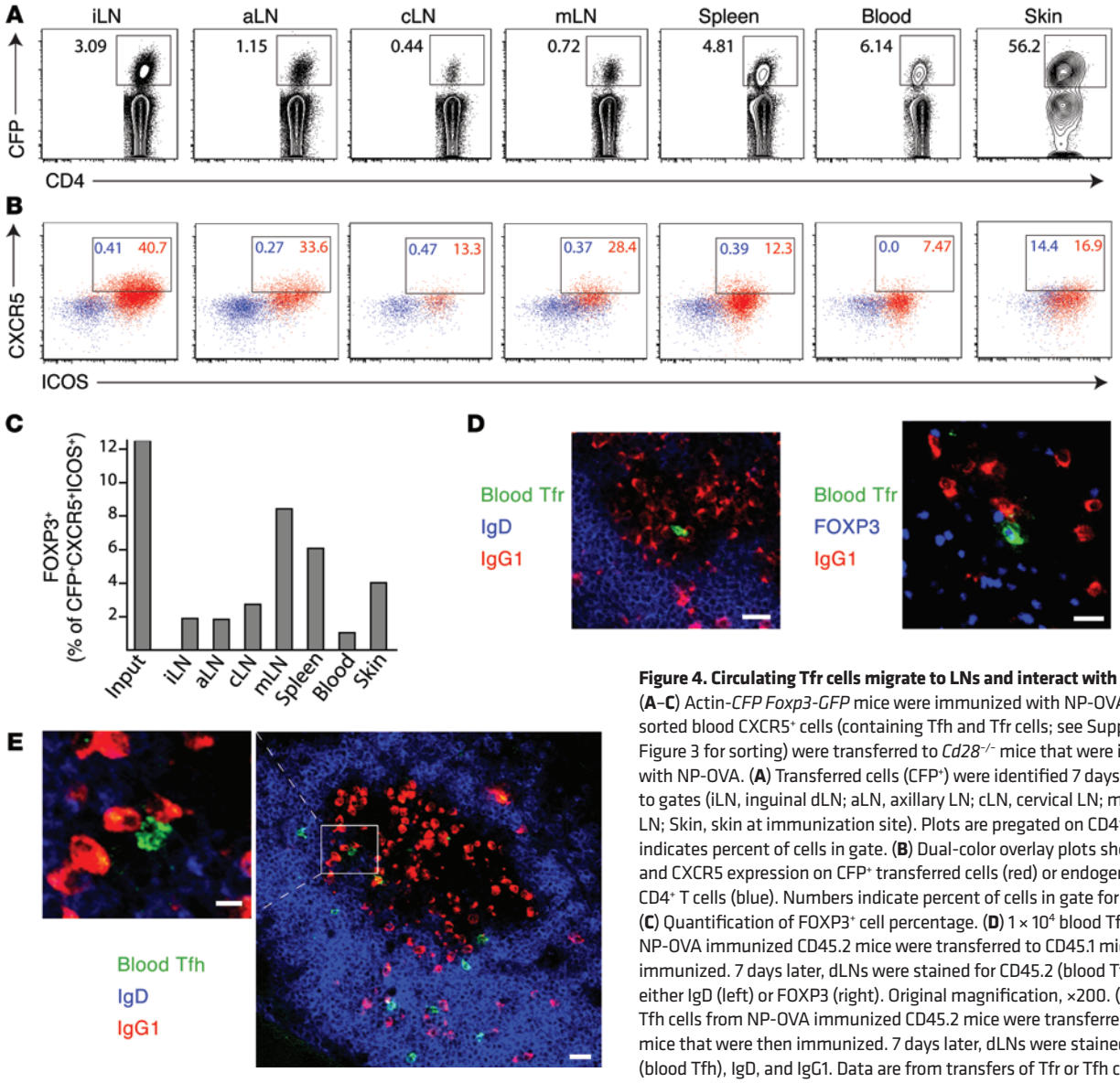

Figure 4. Circulating Tfr cells migrate to LNs and interact with GC B cells. (**A**–**C**) Actin-*CFP Foxp3-GFP* mice were immunized with NP-OVA, and 2×10^4 sorted blood CXCR5$^+$ cells (containing Tfh and Tfr cells; see Supplemental Figure 3 for sorting) were transferred to *Cd28*$^{-/-}$ mice that were immunized with NP-OVA. (**A**) Transferred cells (CFP$^+$) were identified 7 days later according to gates (iLN, inguinal dLN; aLN, axillary LN; cLN, cervical LN; mLN, mesenteric LN; Skin, skin at immunization site). Plots are pregated on CD4$^+$CD19$^-$; number indicates percent of cells in gate. (**B**) Dual-color overlay plots showing ICOS and CXCR5 expression on CFP$^+$ transferred cells (red) or endogenous *Cd28*$^{-/-}$ CD4$^+$ T cells (blue). Numbers indicate percent of cells in gate for each cell type. (**C**) Quantification of FOXP3$^+$ cell percentage. (**D**) 1×10^4 blood Tfr cells from NP-OVA immunized CD45.2 mice were transferred to CD45.1 mice that were immunized. 7 days later, dLNs were stained for CD45.2 (blood Tfr), IgG1, and either IgD (left) or FOXP3 (right). Original magnification, ×200. (**E**) 2×10^4 blood Tfh cells from NP-OVA immunized CD45.2 mice were transferred to CD45.1 mice that were then immunized. 7 days later, dLNs were stained for CD45.2 (blood Tfh), IgD, and IgG1. Data are from transfers of Tfr or Tfh cells sorted from 20 pooled mice into a single recipient and are representative of ≥2 (**A**–**C**) or ≥3 (**D** and **E**) individual experiments. Scale bars: 20 μm; 5 μm (**E**, inset).

s.c. into WT mice, and analyzed Tfr and Tfh cells. We found substantial increases in total CD4$^+$CXCR5$^+$ cells and in the Tfr and Tfh subpopulations in both dLNs and blood compared with mice that did not receive BMDCs (Figure 2, F–H). *Ciita*$^{-/-}$ BMDCs, which are unable to present antigen, were impaired in their ability to stimulate Tfr and Tfh cells in the dLN and blood (Supplemental Figure 2). These findings indicate that DCs are sufficient for development of circulating and blood Tfr and Tfh cells.

Blood Tfr cells recirculate through the blood quickly. We next investigated the cues responsible for exit of Tfr cells from the dLN. Since sphingosine-1-phosphate (S1P) levels control T cell exit into the efferent lymph (23), we tested whether Tfr cells use S1P signals to exit the dLN. We administered FTY720, which prevents cells from responding to S1P (24). Blood Tfr and Tfh cells were virtually absent in mice given FTY720 (Figure 3, A and B). To investigate the kinetics of blood Tfr circulation, we administered FTY720 on day 7 after immunization, at 3 or 6 hours before analysis, and found attenuation of both Tfr and Tfh numbers within a few hours (Figure 3C), demonstrating that these cells exit the blood quickly.

To assess the phenotype of Tfr cells when they exit the dLN, we analyzed Tfr cells in the efferent lymph via thoracic duct cannulation (25). We found similar percentages of Tfr cells in efferent lymph, dLN, and blood (Figure 3, D and E). Tfh cell percentages in efferent lymph were intermediate between those in dLN and blood (Figure 3F). Since ICOS expression is lower on circulating versus dLN Tfr cells, we next investigated whether circulating Tfr cells leave the LN with high ICOS expression or whether low ICOS expression on blood Tfr cells occurs during differentiation. ICOS expression was similar on lymph and blood Tfr cells, but lower than that on dLN Tfr cells (Figure 3G), which suggests that Tfr cells destined to enter the circulation express less ICOS

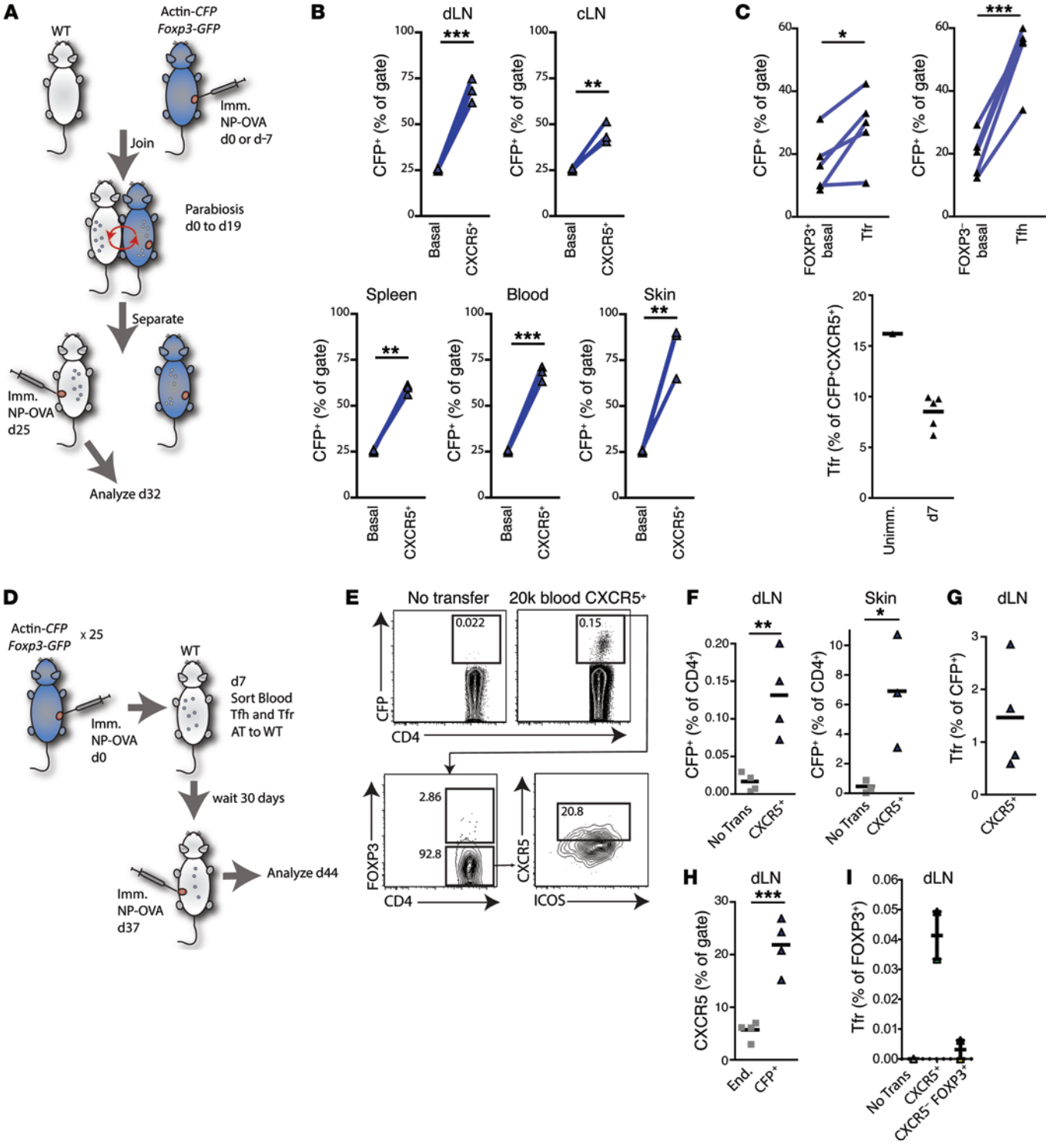

Figure 5. Circulating Tfr and Tfh cells are memory-like cells that persist in vivo. (**A** and **B**) Parabiosis experiments. (**A**) Actin-*CFP Foxp3-GFP* mice were immunized with NP-OVA and surgically joined via parabiosis to WT mice. 6 days after separation, the WT mate was immunized. (**B**) CFP^+ population in basal or $CD4^+CXCR5^+$ populations in the dLN, nondraining cervical LN, spleen, blood, and skin. (**C**) Blood Tfr cells dominated the $CXCR5^+FOXP3^+$ population. Experiments were performed as in **A**, except actin-*CFP Foxp3-GFP* mice were joined with WT *Foxp3-GFP* mice. The indicated populations were analyzed for CFP chimerism and compared with the respective basal populations ($CXCR5^-FOXP3^+$ or $CXCR5^-FOXP3^-$) in the nondraining LN. Comparison of Tfr cell incidence between immunized mice and unimmunized controls is also shown. (**D**–**I**) Memory transfer experiments. Circulating Tfh and Tfr cells persisted for 30 days in vivo. (**D**) 2×10^4 blood $CFP^+ICOS^+CXCR5^+$ (Tfr and Tfh) cells (see Supplemental Figure 3) from blood of immunized mice were transferred to recipients that were immunized 30 days later with NP-OVA. (**E**) Representative plots; number indicates percent of cells in gate. (**F**) CFP^+ cells (percentage of $CD4^+$ T cells) in dLN and in skin at the immunization site. (**G**) Tfr cells (percentage of CFP^+ cells) in dLN. (**H**) CXCR5 expression on CFP^+ cells in dLN. End, endogenous cells. (**I**) Transferred blood $CD4^+$ Treg populations (percentage of total $FOXP3^+$ cells). Data are pooled from 3 (**A** and **B**) or 5 (**C**) replicate surgeries, or pooled from 4 (**D**–**F**) or 2 (**I**) independent transfers. $^*P < 0.05$, $^{**}P < 0.01$, $^{***}P < 0.001$, unpaired Student's *t* test.

during initial differentiation. In addition, expression of Ki67 and CXCR5 was comparable on efferent lymph, blood, and dLN Tfr cells. However, Tfh cell Ki67 and CXCR5 expression in the lymph was similar to that in blood, but less than that in the dLN (Figure 3, H and I). Taken together, these data indicate that circulating Tfr cells resemble lymph Tfr cells, which suggests that the circulating Tfr cell phenotype is acquired during differentiation.

Circulating Tfr cells migrate to diverse LNs and tissues. We next investigated blood Tfr cell trafficking in vivo. To monitor blood Tfr and Tfh cell behavior in vivo, we immunized actin-*CFP Foxp3-GFP* mice with NP-OVA, and 7 days after immunization sorted total $CD4^+ICOS^+CXCR5^+CD19^-$ cells from blood to keep Tfr and Tfh cells in endogenous proportions (Supplemental Figure 3). We transferred these cells into *Cd28*$^{-/-}$ recipients, which were immunized with NP-OVA. We found substantial populations of transferred cells in all LNs tested (Figure 4A), demonstrating that blood Tfr and Tfh cells have homing properties similar to those of central memory cells. Surprisingly, more than half of the $CD4^+$ T cells at the skin immunization site were transferred cells, which demonstrated that circulating Tfr and Tfh cells also can home to peripheral tissues. The transferred cells in the LNs, skin, and blood coexpressed ICOS and CXCR5 (Figure 4B). However, ICOS expression on transferred cells in the blood remained lower, at levels similar to those prior to transfer. Compared with Tfr cells in the blood $CXCR5^+$ population prior to transfer, Tfr cell incidence in the $CXCR5^+CFP^+$ gate in the lymphoid organs was lower, but still present (Figure 4C). Thus, blood Tfr cells can recirculate to many secondary lymphoid organs.

To determine whether circulating Tfr cells can migrate to B cell follicles and become GC Tfr cells, we analyzed the location of transferred cells in the dLNs of WT recipient mice. We immunized CD45.2 WT mice with NP-OVA, sorted blood Tfr cells ($CD4^+ICOS^+CXCR5^+GITR^+CD19^-$, a gating strategy we have validated; Supplemental Figure 3 and ref. 9), and transferred these to WT CD45.1 recipients. We immunized recipients with NP-OVA, and 7 days later found $CD45.2^+$ blood Tfr cells interacting with $IgG1^+$ B cells within GCs (Figure 4D and Supplemental Figure 4). The transferred blood Tfr cells interacted with $IgG1^+$ B cells in the GC, in a manner similar to that exhibited by endogenous LN GC Tfr cells. When we transferred $CXCR5^-ICOS^-$ Tregs from the blood, we could not detect them in the B cell follicles (data not shown). These data indicate that circulating Tfr cells can become GC Tfr cells after secondary exposure to antigen, although it is unclear whether this happens preferentially.

In analogous studies, we transferred blood Tfh cells into WT recipient mice that were subsequently immunized. Transferred blood Tfh cells interacted with $IgG1^+$ class-switched B cells in the interfollicular zone and in the GCs of the dLN of recipient mice (Figure 4E and Supplemental Figure 4). Taken together, these data indicate that circulating Tfr and Tfh cells are capable of migrating to secondary lymphoid organs and can enter GCs to interact with B cells in the GC reaction.

Circulating Tfr and Tfh cells persist in vivo, similar to memory cells. We next investigated whether circulating Tfr cells can persist in vivo, similar to memory T cells. We conducted parabiosis experiments in which the circulatory system from an immunized mouse was surgically joined with that of an unimmunized mouse, allowing exchange of circulating cells — including circulating Tfr and Tfh cells. Following immunization with NP-OVA, actin-*CFP Foxp3-GFP* mice were surgically joined to WT mice (Figure 5A). After being joined for 19 days, chimerism was confirmed, and mice were separated. The WT nonimmunized mate was then immunized, and 7 days later (i.e., at least 32 days since original partner immunization), organs were harvested. To determine whether the circulating $CXCR5^+$ cells from the CFP^+ immunized mouse expanded as memory cells within the WT mate, we compared the basal CFP^+ cell population with that of CFP^+CXCR5^+ cells, reasoning that increases in the CFP^+ contribution in the $CXCR5^+$ population would indicate memory. We defined the percentage of CFP^+ cells (of total $CD4^+ICOS^-CXCR5^-$) in the nondraining (cervical) LN as the basal contribution. Compared with this basal CFP^+ contribution, the CFP^+ contribution in the $CD4^+CXCR5+$ population was significantly enhanced in the dLN (Figure 5B), indicative of memory. We also found substantial increases in the CFP^+CXCR5^+ population in other organs (Figure 5B).

To determine the relative contributions of circulating Tfr cells to increases in CFP^+ cells in the $CXCR5^+$ population, we performed parabiosis experiments as in Figure 5A, but surgically joined actin-*CFP Foxp3-GFP* mice with WT *Foxp3-GFP* mice, in order to track Tregs in both mice. When we compared the CFP^+ Tfr population ($CFP^+CXCR5^+FOXP3^+$) in dLN with the basal $CFP^+CXCR5^-FOXP3^+$ population in the nondraining LN (i.e., baseline Treg chimerism) of WT *Foxp3-GFP* parabiotic mates immunized after separation, we found a significant increase (Figure 5C), which suggests that the circulating Tfr cells may outcompete de novo formed effector GC Tfr cells in the dLN. The increased percentage of CFP^+ Tfh cells in the $CD4^+CXCR5^+FOXP3^-$ population compared with basal chimerism was greater than the increase in CFP^+ Tfr cells in these immunized WT *Foxp3-GFP* parabiotic mates. The Tfr percentage of all CFP^+CXCR5^+ cells was decreased in immunized compared with unimmunized WT *Foxp3-GFP* parabiotic mates (Figure 5C). This relative reduction in Tfr cells may promote initiation of the secondary response in the circulating memory $CXCR5^+$ Tfh cells, since the Tfr/Tfh ratio can control antibody production (9).

Although parabiosis experiments are advantageous because circulating cells can be transferred over time without loss from harvesting procedures, it is possible that $CXCR5^-FOXP3^+$ memory cells may differentiate into Tfr cells in the dLN after antigen exposure. Therefore, we used a complementary approach: we transferred blood $CXCR5^+$ cells sorted from NP-OVA–immunized actin-*CFP Foxp3-GFP* mice into WT recipient mice (Figure 5D). After 30 days, WT recipients were immunized with NP-OVA, and dLNs were harvested 7 days later. We found a small, but substantial, population of CFP^+ cells in the dLN and skin (Figure 5, E and F). Although most CFP^+CXCR5^+ cells were Tfh cells, there was a small Tfr population (Figure 5G). The CFP^+ cells that persisted had high levels of CXCR5 (Figure 5H), which suggests that many of these cells maintained their follicular phenotype. Importantly, transferred $CXCR5^-ICOS^-FOXP3^+$ blood cells (i.e., non-Tfr Tregs) could not persist in vivo (Figure 5I), which suggests that memory-like properties are unique to Tfr cells. However, it is important to note that we did not test $CXCR5^-ICOS^+$ Tregs, nor Tregs from tissues, which may contain other Treg memory populations. Together, these data indicate that circulating Tfr — and Tfh — cells can recirculate throughout the body for long periods of time and regulate the GC reaction after secondary exposure to antigen.

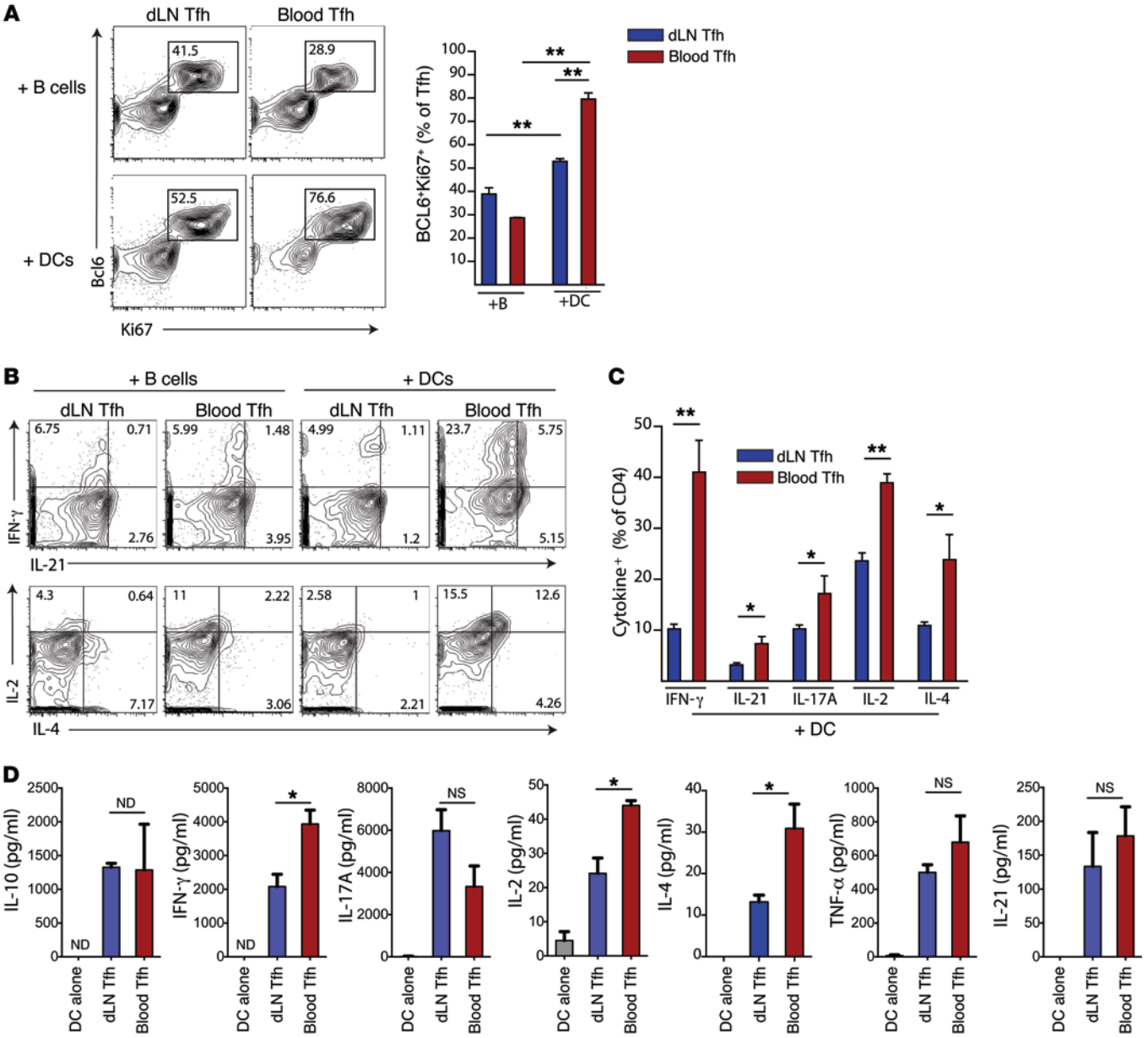

Figure 6. Circulating Tfh cells require DCs for enhanced cytokine production. (**A**) In vitro activation assay. dLN or blood Tfh cells (sorted as $CD4^+ICOS^+CXCR5^+GITR^-CD19^-$; see Supplemental Figure 3) were plated with B cells or $CD11c^+MHCII^+$ DCs (sorted from dLN of WT immunized mice) plus anti-IgM and anti-CD3 for 6 days. Left: Plots pregated on $CD4^+CD19^-$; number indicates percent of cells in gate. Right: Quantification of $BCL6^+Ki67^+$ cells. (**B** and **C**) Intracellular cytokine staining of Tfh cells from cocultures with B cells or DCs as in **A**, except samples were stimulated with PMA/ionomycin for 4 hours in the presence of Golgistop prior to staining. (**B**) Representative plots; numbers indicate percentage of cells in the each respective quadrant. (**C**) Quantification. (**D**) Quantification of cytokines measured in culture supernatants of cultures as in **A**. ND, not detected. Graphs represent mean ± SEM of pooled data from 3 independent experiments. $^*P < 0.05$, $^{**}P < 0.01$, $^{***}P < 0.001$, unpaired Student's *t* test (**C** and **D**) or 1-way ANOVA with Tukey post-test (**A**).

Circulating memory-like Tfh cells require DCs for enhanced cytokine production. We next analyzed the reactivation requirements for memory-like Tfh cells, using in vitro systems to investigate which APCs are necessary for their reactivation. We immunized WT mice with NP-OVA and sorted dLN effector and circulating memory-like Tfh cells. We compared the reactivation of these cells after culture with B cells or DCs sorted from same dLNs. Culture of dLN Tfh cells with B cells led to a higher percentage of $BCL6^+Ki67^+$ cells than culture of circulating Tfh cells with B cells (Figure 6A). Culture of dLN Tfh cells with DCs only modestly increased the percentage of $BCL6^+Ki67^+$ cells. In contrast, culture of circulating Tfh cells with DCs led to a greatly increased percentage of $BCL6^+Ki67^+$ cells, compared with circulating Tfh cells cultured with B cells or with dLN Tfh cells cultured with DCs (Figure 6A). Therefore, DCs can stimulate enhanced activation of circulating Tfh cells.

We next investigated whether the increased activation of circulating Tfh cells cultured with DCs resulted in greater cytokine production. We found increases in staining for IFN-γ, as well as smaller increases in staining for IL-21, IL-17A, IL-2, and IL-4, in circulating Tfh cells cultured with DCs (Figure 6, B and C). We

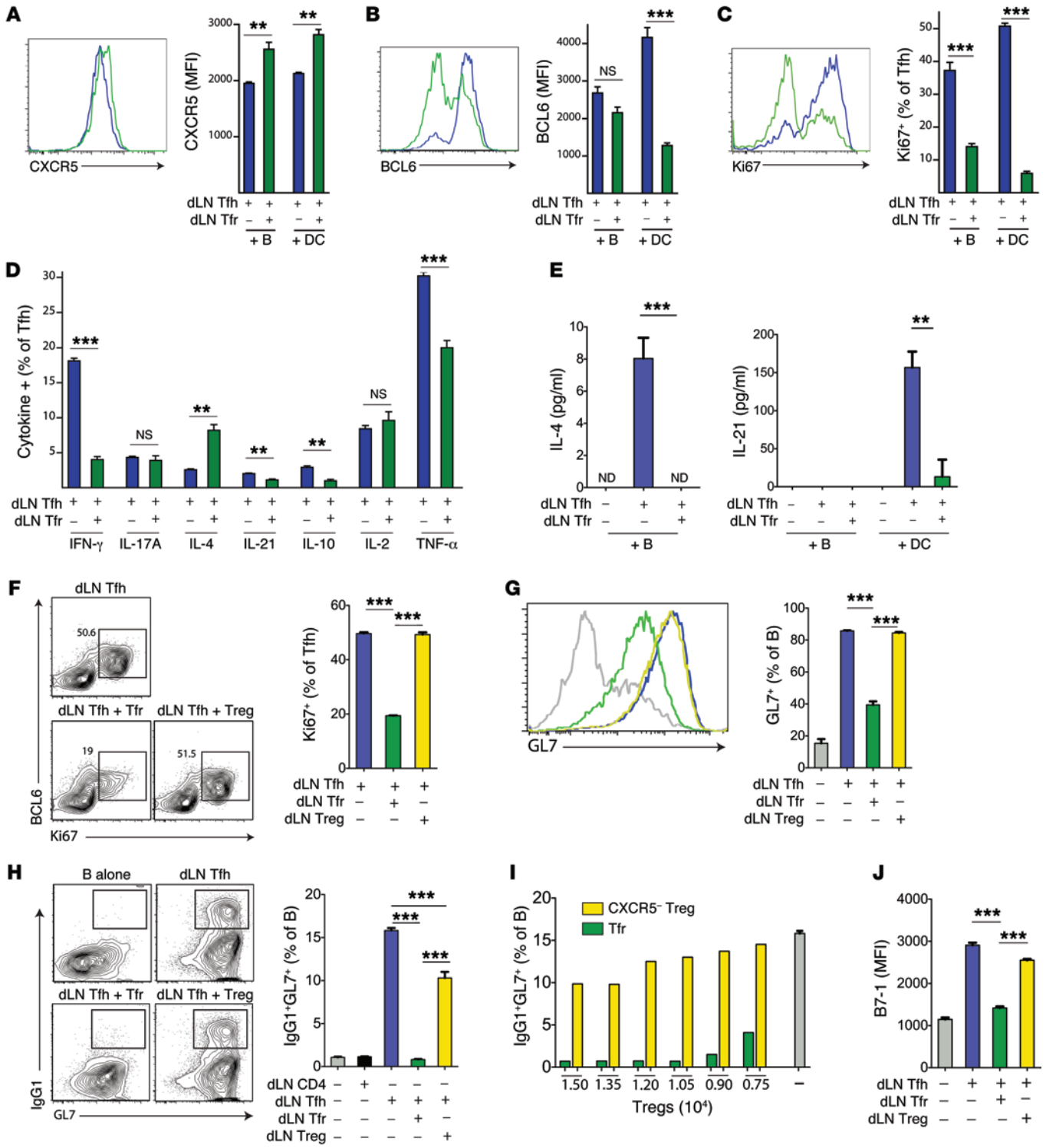

Figure 7. Tfr cells suppress Tfh and B cells. (**A**–**E**) dLN Tfr suppression assays. 3 × 10^4 dLN Tfh cells ($CD4^+ICOS^+CXCR5^+GITR^-CD19^-$; see Supplemental Figure 3) were plated with 1.5 × 10^4 Tfr cells ($CD4^+ICOS^+CXCR5^+GITR^+CD19^-$) and either 5 × 10^4 B cells or 5 × 10^4 DCs (isolated from the dLN of WT immunized mice) for 5–6 days with anti-CD3 and anti-IgM. (**A**) Tfh cells were gated as $CD4^+CD19^-FOXP3^-$ and stained for CXCR5. (**B** and **C**) Tfh cells (cultured and gated as in **A**) were intracellularly stained for (**B**) BCL6 or (**C**) Ki67. (**D**) Intracellular cytokine staining in Tfh cells from suppression assays with B cells. (**E**) Quantification of IL-4 and IL-21 in culture supernatants. (**F**–**J**) 3 × 10^4 Tfh cells ($CD4^+ICOS^+CXCR5^+FOXP3^-CD19^-$) and 5 × 10^4 B cells were plated with 1.5 × 10^4 Tfr cells ($CD4^+ICOS^+CXCR5^+FOXP3^+CD19^-$) or 1.5 × 10^4 conventional dLN Tregs ($CD4^+ICOS^-CXCR5^-FOXP3^+$) for 6 days. (**F**) Ki67 in Tfh cells from cultures. Left: Plots pregated on $CD4^+FOXP3^-CD19^-$; number indicates percent of cells in gate. Right: Quantification. (**G**) B cells were quantified for GL7 expression. (**H**) IgG1 expression in B cells. (**I**) Dose response of suppression of IgG1 expression in B cells cultured as indicated. (**J**) B7-1 expression on B cells. Data are mean ± SEM of 3–4 replicate wells and are representative of 3 independent experiments. *P < 0.05, **P < 0.01, ***P < 0.001, unpaired Student's t test (**A**–**E**) or 1-way ANOVA with Tukey post-test (**F**–**J**).

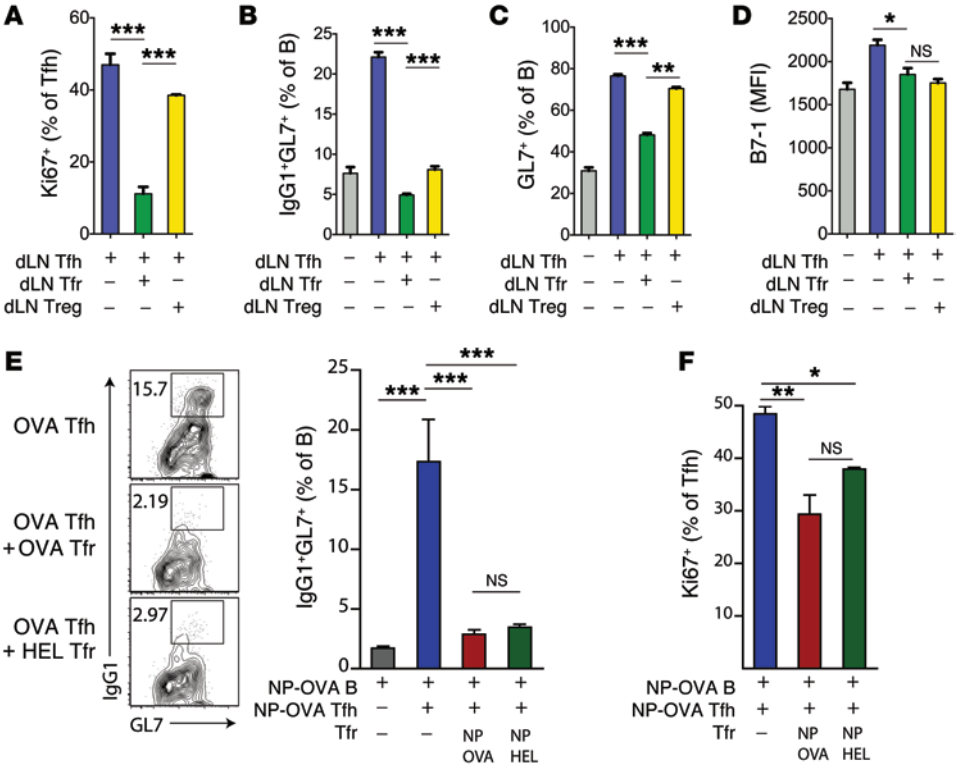

Figure 8. Tfr cells can suppress GC B cells and do not require specific antigen for suppressive capacity. (**A**–**D**) Tfr cells suppress GC B cells. 3 × 10^4 Tfh cells and 1.5 × 10^4 Tfr cells or 1.5 × 10^4 non-Tfr Tregs (see Supplemental Figure 3) were cultured with 5 × 10^4 GC B cells (sorted as $CD19^+GL7^+CD4^-$ from the dLN of WT mice immunized 12 days previously with NP-OVA) in the presence of NP-OVA for 6 days. (**A**) Quantification of $Ki67^+$ Tfh cells. (**B**) Quantification of $IgG1^+GL7^+$ B cells. (**C**) Quantification of $GL7^+$ B cells. (**D**) Quantification of B7-1 expression on B cells. (**E** and **F**) In vitro antigen-specific suppression assays. 3 × 10^4 Tfh and 5 × 10^4 total B cells from the dLN of NP-OVA immunized mice were cultured with 1.5 × 10^4 dLN Tfr cells (sorted as $CD4^+ICOS^+CXCR5^+GITR^+CD19^-$) from either NP-OVA– or NP-HEL–immunized mice in the presence of NP-OVA for 6 days. (**E**) B cell GL7 and IgG1 expression. Left: Representative plots pregated on $CD19^+IA^+$; number indicates percent of cells in gate. Right: Quantification. (**F**) Quantification of $Ki67^+$ Tfh cells. Data indicate mean ± SEM of 3–4 replicate wells and are representative of 3 independent experiments. *$P < 0.05$, **$P < 0.01$, ***$P < 0.001$, 1-way ANOVA with Tukey post-test.

also found increased IFN-γ, IL-2, and IL-4, but not TNF-α, IL-21, or IL-17A, in culture supernatants (Figure 6D). Thus, circulating memory-like Tfh cells can be reactivated by DCs, resulting in heightened cytokine production.

Effector Tfr cells potently suppress Tfh and B cells. To compare the suppressive functions of circulating memory-like and effector Tfr cells, we first investigated how dLN effector Tfr cells suppress B cells. We cultured dLN Tfh cells with dLN Tfr cells and total B cells or DCs for 6 days in the presence of anti-CD3 and anti-IgM. Addition of Tfr cells did not result in downregulation of CXCR5 on Tfh cells (Figure 7A), which suggests that Tfr cells do not divert Tfh cells away from the GC. BCL6 expression in the Tfh cells was attenuated profoundly in the presence of Tfr cells and DCs, but not B cells (Figure 7B). Moreover, Tfh Ki67 expression was strongly suppressed by Tfr cells in both B cell and DC culture conditions (Figure 7C), which suggests that a key mechanism of effector Tfr cell suppression is the inhibition of Tfh cell cycling.

We next examined whether Tfr cells also suppress Tfh cell cytokine production. We found that Tfr cells suppressed IFN-γ, IL-21, IL-10, and TNF-α expression by Tfh cells cultured with B cells (Figure 7D), and expression of IFN-γ, IL-10, and TNF-α in culture supernatants (Supplemental Figure 5). We did not detect IL-21 in the cultures when B cells were used, but detected low levels of IL-21 when DCs were used, which was suppressed by Tfr cells (Figure 7E). Strikingly, IL-4 and IL-2 in the culture supernatants were also greatly suppressed by the addition of Tfr cells (Figure 7E and Supplemental Figure 5).

Next, we determined whether conventional Tregs suppress Tfh cell activation, as Tfr cells did, by comparing the suppressive capacity of conventional Tregs ($CD4^+ICOS^-CXCR5^-FOXP3^+CD19^-$) with that of Tfr cells. The cell cycle marker Ki67 was attenuated in Tfh cells when Tfr cells were added, but not when conventional Tregs were added (Figure 7F), which suggests that Tfr cell suppression depends on a follicular program.

We next investigated whether effector Tfr cells also affect B cell function. The GC B cell marker GL7 was upregulated on B cells when cultured with Tfh cells, but markedly reduced when Tfr cells were present (Figure 7G). In contrast, conventional Tregs did not reduce GL7 expression. Importantly, whereas Tfh cells stimulated robust class switch recombination in B cells, this was potently inhibited by Tfr cells (Figure 7H). Conventional Tregs only modestly inhibited class switch recombination, even at higher Treg ratios (Figure 7, H and I). Tfh cell–stimulated B7-1 expression was also attenuated by Tfr cells, but not by conventional Tregs (Figure 7J). These data indicate that LN Tfr cells, but not conventional Tregs, have the capacity to suppress Tfh and B cells responses by

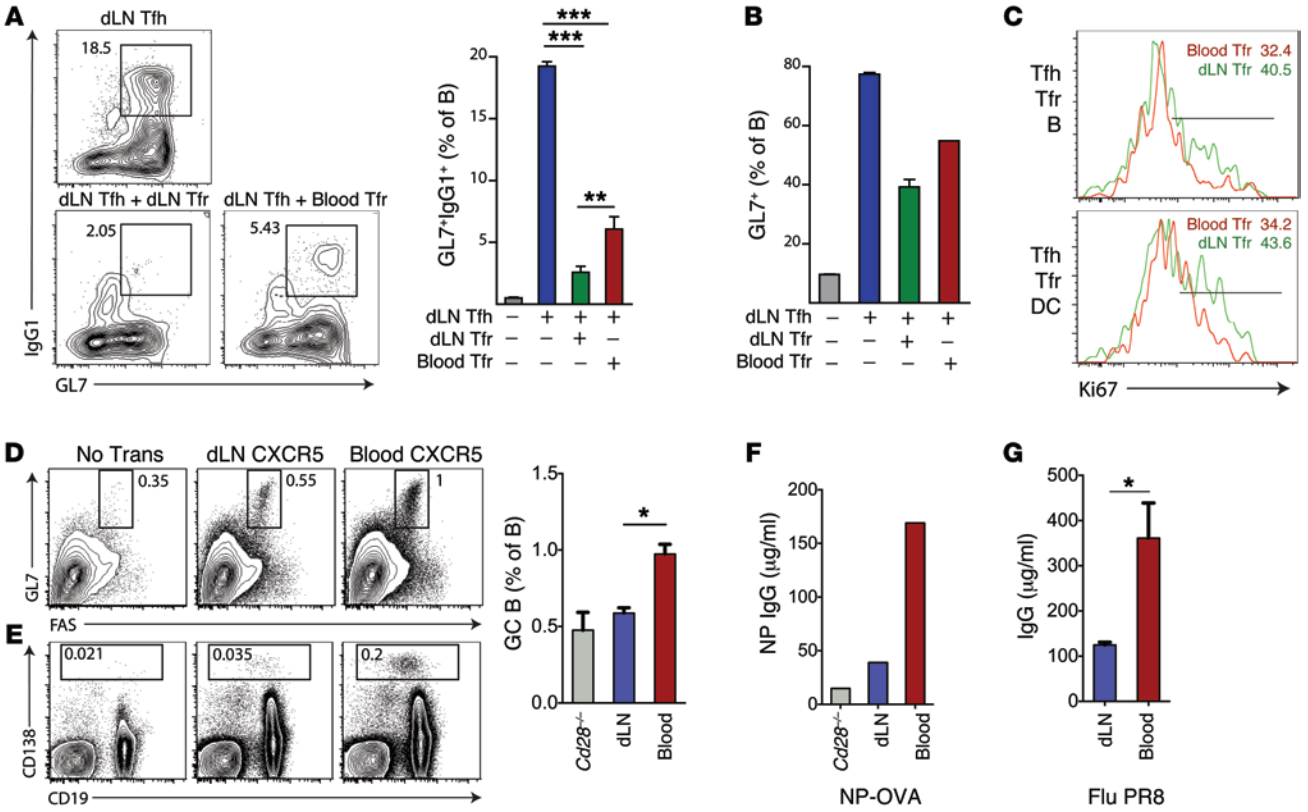

Figure 9. Circulating Tfr cells have lower suppressive capacity. (**A**–**C**) Suppression assays. Tfr cells (CD4$^+$ICOS$^+$CXCR5$^+$GITR$^+$CD19$^-$; see Supplemental Figure 3) were cultured with dLN Tfh cells and B cells. (**A**) GL7 and IgG1 expression on B cells. Left: Plots pregated on CD19$^+$IA$^+$; number indicates percent of cells in gate. Right: Quantification. (**B**) Quantification of GL7$^+$ B cells. (**C**) Ki67 staining in Tfr cells. Histograms are pregated on CD4$^+$CD19$^-$FOXP3$^+$; number indicates percent of cells in gate. (**D** and **E**) Blood Tfh and Tfr cells elicit more potent B cell responses. 2 × 10^4 blood or dLN CD4$^+$ICOS$^+$CXCR5$^+$ cells (Tfh and Tfr) from actin-*CFP Foxp3-GFP* mice were transferred to *Cd28*$^{-/-}$ mice that were immunized. dLNs were harvested, and B cells were stained for (**D**) GL7 and FAS (pregated on CD19$^+$) or (**E**) CD138 and CD19 (pregated on live cells). Left: Representative plots; number indicates percent of cells in gate. Right: Quantification of GC B cells. (**F**) Similar experiments as in **D**, except serum was collected on d10 after transfer. (**G**) Mice were infected with influenza PR8 virus, and blood or dLN CD4$^+$ICOS$^+$CXCR5$^+$ cells were transferred to *Cd28*$^{-/-}$ mice and infected with PR8 influenza. Serum IgG was measured 12 days later. Data are mean ± SEM of pooled data from 3 (**A**, **B**, and **D**) or 2 (**G**) independent experiments or are representative of 3 independent experiments (**C** and **F**). $^*P < 0.05$, $^{**}P < 0.01$, $^{***}P < 0.001$, unpaired Student's *t* test (**G**) or 1-way ANOVA with Tukey post-test (**A** and **D**).

inhibiting Tfh cell activation and cytokine production as well as B cell activation and class switch recombination.

Effector Tfr cells do not require specific antigen to suppress. Next, we investigated whether dLN effector Tfr cells suppress activated/differentiated GC-like B cells. We cultured GL7$^+$ B cells with dLN Tfh cells and either dLN Tfr cells or conventional Tregs (all sorted as in Figure 7F) in the presence of NP-OVA for 6 days. Tfr cells were able to suppress Ki67 in Tfh cells, but CXCR5$^-$ICOS$^-$ Tregs exhibited only modest suppression (Figure 8A). Furthermore, there were large percentages of IgG1$^+$GL7$^+$ class-switched B cells in dLN Tfh and GL7$^+$ B cell cocultures, which were substantially reduced by addition of dLN Tfr cells, and attenuated to a lesser degree by conventional Tregs (Figure 8B). In contrast, the percentages of GL7$^+$ B cells in these cultures were greatly suppressed by Tfr cells, but not substantially by conventional Tregs (Figure 8C). B7-1 was modestly attenuated on GL7$^+$ B cells by both Tfr cells and conventional Tregs, to a similar extent (Figure 8D). These data indicate that Tfr cells have the capacity to suppress GL7$^+$ B cells after they have already been activated.

Next, we investigated whether specific antigen is required for the suppressive capacity of Tfr cells. We sorted Tfr cells from dLNs of mice immunized with NP-OVA or NP-HEL, then cultured the sorted cells with Tfh and B cells from dLNs of mice immunized with NP-OVA. We added NP-OVA to the wells to stimulate linked recognition. Both NP-OVA– and NP-HEL–generated Tfr cells potently suppressed B cell class switch recombination (Figure 8E). Likewise, both groups of Tfr cells similarly suppressed Ki67 in Tfh cells (Figure 8F). Thus, LN Tfr cells can suppress differentiated GC B cells, and suppression does not require antigen-specific Tfr cells.

Circulating memory-like Tfr cells have less suppressive capacity. Finally, we compared the abilities of dLN and circulating Tfr cells to suppress dLN effector Tfh and B cells. Circulating Tfr cells suppressed IgG1 in B cells, but less potently than did dLN Tfr cells (Figure 9A). Similarly, circulating Tfr cells reduced GL7 in B cells, but less robustly than dLN Tfh cells (Figure 9B). Thus, circulating Tfr cells suppress B cells by a mechanism similar to that of dLN Tfh cells, but to a lesser extent. Additionally, Ki67 expression was observed in a lower percentage of circulating than dLN Tfr cells, regardless of culture with B cells or DCs (Figure 9C). Therefore, circulating Tfr cells are less potently activated by DCs than are dLN Tfr cells.

Because circulating memory-like Tfh cells were more potent than effector Tfh cells, and circulating memory-like Tfr cells were

less inhibitory than effector Tfr cells in vitro, we postulated that there would be differences in the effects of the total circulating and dLN CXCR5$^+$ populations (which contain both Tfr and Tfh cells) on B cell activation in vivo. We sorted total CXCR5$^+$ cells from dLNs or blood of NP-OVA immunized mice and transferred these cells to *Cd28*$^{-/-}$ recipients that were immunized with NP-OVA. We detected a greater percentage of dLN GC B cells, plasma cells, and serum NP-specific antibody 10 days after immunization of the recipients of blood CXCR5$^+$ cells (Figure 9, D–F). We performed similar transfer experiments with mice infected with influenza. We infected mice with influenza i.n. and transferred dLN or blood CXCR5$^+$ cells to *Cd28*$^{-/-}$ recipients that were then infected with influenza. After 13 days, we found enhanced IgG in the serum of recipients of blood versus dLN CXCR5$^+$ cells (Figure 9G). Together, these data demonstrate that blood CXCR5$^+$ cells are able to stimulate enhanced B cell responses compared with dLN CXCR5$^+$ cells.

Discussion

In this study, we demonstrated that circulating Tfr and Tfh cells differ from dLN effector Tfr and Tfh cells and possess immunological memory-like functions. We hypothesize that the decreased suppressive capacity of circulating Tfr cells permits a strong memory response by circulating Tfh cells. Our data therefore point to a novel mechanism of control of secondary antibody responses in which circulating memory-like Tfr and Tfh cells enable rapid recall responses upon reencounter of antigen.

Based on our findings, we hypothesize that 2 fates emerge for follicular CD4$^+$FOXP3$^+$ cells after antigen presentation by DCs. Subsets of Tfr cells that have medium-to-low CXCR5 and low CD69 expression exit the LN via S1P gradients, destined to become circulating memory-like Tfr cells. Tfr cells with high CXCR5 and CD69 expression follow CXCL13 gradients to the B cell zone, where full differentiation of the effector program occurs. Importantly, when Tfr cells entered the lymph, they already exhibited a phenotype similar to that of circulating Tfr cells, which suggests that the memory-like Tfr cell phenotype is acquired during differentiation. This hypothesis is supported by a recent study demonstrating that GC Tfh cells can move between the GC and interfollicular regions, but do not enter the circulation (18), and another report that circulating Tfh cells, unlike LN Tfh cells, do not require SAP (or, consequently, B cells) for differentiation (15).

Far less is known about the signals necessary for Tfr function than those for Tfr differentiation (26). It has been suggested that there are specialized subsets of effector Tregs that use Th cell transcription factors not normally expressed by Tregs to position themselves in specific locations to help program Th-specific suppression (26). CXCR5$^-$ FOXP3$^+$ Tregs from immunized mice were much less potent or unable to suppress GL7, B7-1, or class switching to IgG1 in vitro compared with LN Tfr cells. The inability of conventional Tregs to suppress B cells in vitro suggests a Tfr cell program — beyond CXCR5 expression and distinct T and B cell zones directed by CXCL13 gradients — that is essential for Tfr cell–suppressive functions. We hypothesize that the similar expression of transcription factors (such as BCL6) in Tfh and Tfr cells may be key to this Tfr cell suppression program.

We identified several mechanisms by which Tfr cells suppress B cell responses. We found that LN effector (and circulating) Tfr cells potently suppressed activation of Tfh cells. LN effector Tfr cells potently suppressed production of cytokines by effector Tfh cells as well as dLN effector Tfh cell–mediated B cell activation and class switch recombination. Interestingly, we found that effector LN Tfr cells suppressed B cell responses in an antigen-independent fashion. Therefore, previously existing Tfr cells may be able to alter differentiating Tfh cells specific for new antigens.

It is not currently known whether Tregs can possess immunological memory. One report showed that self-reactive Tregs can have regulatory memory within the skin (27). It is also unclear whether these putative memory Tregs have memory properties similar to those of conventional CD4$^+$ memory cells or unique characteristics related to the Treg program. Our present findings suggest that circulating Tfr cells have central memory-like properties and can recirculate from the blood to secondary lymphoid organs and tissues quickly, on the order of hours.

Circulating memory-like Tfr cells were more abundant than were effector/GC Tfr cells after secondary exposure to antigen in parabiosis experiments, which suggests that circulating Tfr cells may function to control the fate of GC responses more potently than newly differentiated effector Tfr cells. We hypothesize that the main role of circulating memory Tfr cells is to ensure proper memory Tfh and B cell activation, thereby limiting inappropriate antibody responses. The proportionately higher percentage of CFP$^+$CXCR5$^+$ Tfr cells observed in unimmunized WT parabiotic mice supports this hypothesis. Circulating memory Tfr cells may also prevent autoimmunity by raising the threshold for B cell activation. During secondary antigen exposure, suppression by circulating memory-like Tfr cells can be surmounted by circulating memory-like Tfh cells, which expand greatly and are more potent compared with dLN effector Tfh cells, thereby enabling productive recall antibody responses.

Since circulating memory-like Tfr cells require distinct cues compared with LN effector Tfr cells, it is likely that these cells are programmed differently. We showed herein that although both dLN and circulating Tfr cells suppressed B cells, the circulating Tfr cells exhibited lower suppressive capacity. Understanding how Tfr cells control humoral responses should provide insights that enable new strategies for developing long-lasting B cell memory to vaccines and for controlling pathogenic B cell responses by modulating Tfr cells.

Methods

Mice. WT C57BL/6, *Ciita*$^{-/-}$, *Itax*-DTR (CD11c-DTR), *Ighm*$^{-/-}$ (μMT), actin-*CFP*, and *Cd28*$^{-/-}$ mice were from The Jackson Laboratory. Actin-*CFP Foxp3-GFP* mice were generated by crossing actin-*CFP* mice with *Foxp3-IRES-GFP* (*Foxp3-GFP*) mice (28). For CD11c-DTR experiments, 1 μg DT (Sigma-Aldrich) was injected i.p. every 2 days starting at day 0 (d0) after immunization, and cells were harvested on d7. In some experiments, WT mice were injected i.p. with 25 mg/kg FTY720 (Cayman Chemical), either every 2 days starting at d2 after immunization or at 3 or 6 hours before harvesting organs. Thoracic duct cannulation was performed as described previously (25).

Immunizations and infections. For NP-OVA or NP-HEL immunization, 100 μg NP_{18}-OVA or NP-HEL (Biosearch Technologies) in a 1:1 H37RA CFA (DIFCO) emulsion was injected s.c. on the mouse flanks. For influenza studies, mice were infected i.n. with 0.5 LD_{50} PR8 influenza. For LCMV studies, mice were infected i.v. with 4×10^6 PFU LCMV Clone 13. At d7–d10 after immunization or infection, mouse

dLNs or spleen were harvested, blood was collected via cardiac puncture, and immune cells were isolated by sucrose density centrifugation using Lymphocyte Separation Media (LSM; MPbio).

BMDCs. BMDCs were prepared by culturing BM cells from WT or *Ciita*$^{-/-}$ mice with 30 ng/ml GM-CSF (Peprotech) for 7 days. During the last 24 hours, 20 ng/ml LPS (Sigma-Aldrich) and 20 μg/ml NP-OVA were added. 1×10^6 cells were injected s.c. into the flank of WT mice.

Flow cytometry. Cells were stained with antibodies from Biolegend (anti-CD4, RM4-5; anti-ICOS, 15F9; anti-CD19, 6D5; anti-CD69, H1.2F3; anti-CD11c, N418; anti–MHCII, M5/114.15.2; anti–IL-17A, TC11-18H10.1; anti–IL-2, JES6-5H4; anti–IFN-γ, XMG1.2; anti–IL-4, 11B11; anti–TNF-α, MP6-XT22; anti-CD138, 281-2), eBioscience (anti-FOXP3, FJK-16S; anti-BCL6, mGI191E; anti–IL-21, FFA21), BD Biosciences (anti-GL7; anti-Ki67, B56; anti-IgG1, A85-1), and Abcam (goat anti-GFP). For CXCR5 staining, biotinylated anti-CXCR5 (2G8; BD Biosciences) was used followed by BV421- or APC-conjugated streptavidin (Biolegend). For intracellular staining, FOXP3 fix/perm kit was used (eBioscience). For intracellular cytokine staining, cells were preincubated with 1 μg/ml ionomycin (Sigma-Aldrich), 500 ng/ml PMA (Sigma-Aldrich), and Golgistop (BD Biosciences) for 4 hours. Flow cytometry was analyzed with an LSR II instrument (BD Biosciences). For cell sorting, CD4$^+$ T cells were pre-enriched with anti-CD4 microbeads (Miltenyi Biotec). All cell sorting (see Supplemental Figure 3 for gates) was performed on an AriaII special order system (BD Biosciences).

Adoptive transfers. For CXCR5$^+$ T cell transfers, 20 actin-*CFP Foxp3-GFP* or WT mice were immunized s.c. with NP-OVA or infected i.n. with influenza as described above, and dLN or blood was collected 7 days later. 2×10^4 CFP$^+$CD4$^+$ICOS$^+$CXCR5$^+$ cells were adoptively transferred to *Cd28*$^{-/-}$ or WT mice that were then immunized s.c. with NP-OVA in CFA or infected i.n. with virus. For memory experiments, recipients were rechallenged with antigen on d30 after initial immunization, and organs were harvested 7 days later. Transferred cells were identified by either CFP expression or FOXP3 GFP expression by intracellular staining with an anti-GFP polyclonal antibody (Abcam).

Parabiosis. For parabiosis, mice were anesthetized and surgically joined as described previously (25). Parabiosis was confirmed by analyzing blood CFP chimerism. Mice were separated after 19 days and immunized s.c. on the nonjoined side 6 days later. Contributions of partner-derived circulating cells were calculated as the average of the percent of CFP$^+$ cells in the WT mouse in the nondraining cervical LNs.

In vitro suppression assay. Cells were counted on an Accuri cytometer (BD Biosciences). For Tfh cell stimulation assays, 2×10^4 dLN or blood Tfh cells (CD4$^+$ICOS$^+$CXCR5$^+$GITR$^-$CD19$^-$; see Supplemental Figure 3) were plated with 5×10^4 B cells (CD19$^+$) or 2×10^4 DCs (CD3$^-$CD19$^-$CD11c$^+$), all purified from dLNs of WT mice immunized with NP-OVA 7 days previously. For DCs, dLNs were digested with 500 U/ml collagenase I (Worthington Biochemical) before isolation. Tfh plus B cells or DCs were cultured with 2 μg/ml soluble anti-CD3 (2C11; BioXcell) and 5 μg/ml anti-IgM (Jackson Immunoresearch Laboratories) for 5–6 days. For Tfr suppression assays, 1×10^4 Tfr cells (CD4$^+$ICOS$^+$CXCR5$^+$GITR$^+$CD19$^-$) from either dLN or blood of WT mice immunized with NP-OVA 7 days previously were added to the wells, and cells were harvested 6 days later. Cytokine concentrations were measured by Cytometric Bead Array (BD Bioscience).

Confocal microscopy. Confocal microscopy was performed as described previously (9). Briefly, organs were embedded in OCT medium (Tissue-Tek). 10-μm sections were cut, fixed, and stained using the FOXP3 kit (eBioscience). Samples were imaged using an Olympus confocal microscope with a ×20 objective.

Statistics. For single comparisons, unpaired, 2-tailed Student's *t* test was used; for multiple comparisons, 1-way ANOVA with Tukey post-test was used. Data represent mean ± SD or SEM as indicated. A *P* value less than 0.05 was considered significant.

Study approval. All mice were used according to the Harvard Medical School Standing Committee on Animals and NIH guidelines.

Acknowledgments

We thank C. Armet for technical help and E.J. Wherry for virus reagents. This work was supported by the NIH through grants T32HL007627 (to P.T. Sage), T32HL066987 (to D. Alvarez), R37AI38310 and P01AI56299 (to A.H. Sharpe), and P01AI078897 (U.H. von Andrian, PPG PI; A.H. Sharpe, Project 2 PI).

Address correspondence to: Arlene H. Sharpe, NRB 77 Avenue Louis Pasteur, Room 837, Boston, Massachusetts 02115, USA. Phone: 617.432.6568; E-mail: Arlene_Sharpe@hms.harvard.edu.

1. Breitfeld D, et al. Follicular B helper T cells express CXC chemokine receptor 5, localize to B cell follicles, and support immunoglobulin production. *J Exp Med*. 2000;192(11):1545–1552.
2. Crotty S. Follicular helper CD4 T cells (TFH). *Annu Rev Immunol*. 2011;29:621–663.
3. Nurieva RI, et al. Generation of T follicular helper cells is mediated by interleukin-21 but independent of T helper 1, 2, or 17 cell lineages. *Immunity*. 2008;29(1):138–149.
4. Johnston RJ, et al. Bcl6 and Blimp-1 are reciprocal and antagonistic regulators of T follicular helper cell differentiation. *Science*. 2009;325(5943):1006–1010.
5. Nurieva RI, et al. Bcl6 mediates the development of T follicular helper cells. *Science*. 2009;325(5943):1001–1005.
6. Linterman MA, et al. Foxp3$^+$ follicular regulatory T cells control the germinal center response. *Nat Med*. 2011;17(8):975–982.
7. Chung Y, et al. Follicular regulatory T cells expressing Foxp3 and Bcl-6 suppress germinal center reactions. *Nat Med*. 2011;17(8):983–988.
8. Wollenberg I, et al. Regulation of the germinal center reaction by Foxp3$^+$ follicular regulatory T cells. *J Immunol*. 2011;187(9):4553–4560.
9. Sage PT, Francisco LM, Carman CV, Sharpe AH. The receptor PD-1 controls follicular regulatory T cells in the lymph nodes and blood. *Nat Immunol*. 2013;14(2):152–161.
10. Morita R, et al. Human blood CXCR5(+) CD4(+) T cells are counterparts of T follicular cells and contain specific subsets that differentially support antibody secretion. *Immunity*. 2011;34(1):108–121.
11. Schaerli P, Willimann K, Lang AB, Lipp M, Loetscher P, Moser B. CXC chemokine receptor 5 expression defines follicular homing T cells with B cell helper function. *J Exp Med*. 2000;192(11):1553–1562.
12. Rasheed AU, Rahn HP, Sallusto F, Lipp M, Muller G. Follicular B helper T cell activity is confined to CXCR5(hi)ICOS(hi) CD4 T cells and is independent of CD57 expression. *Eur J Immunol*. 2006;36(7):1892–1903.
13. Fazilleau N, et al. Lymphoid reservoirs of antigen-specific memory T helper cells. *Nat Immunol*. 2007;8(7):753–761.
14. Hale JS, et al. Distinct memory CD4$^+$ T cells with commitment to T follicular helper- and T helper 1-cell lineages are generated after acute viral infection. *Immunity*. 2013;38(4):805–817.
15. He J, et al. Circulating precursor CCR7(lo)PD-1(hi) CXCR5(+) CD4(+) T cells indicate Tfh cell activity and promote antibody responses upon antigen reexposure. *Immunity*. 2013;39(4):770–781.
16. Bossaller L, et al. ICOS deficiency is associated with a severe reduction of CXCR5+CD4 germinal center Th cells. *J Immunol*. 2006;177(7):4927–4932.
17. Bauquet AT, et al. The costimulatory molecule

ICOS regulates the expression of c-Maf and IL-21 in the development of follicular T helper cells and TH-17 cells. *Nat Immunol*. 2009;10(2):167–175.
18. Shulman Z, et al. T follicular helper cell dynamics in germinal centers. *Science*. 2013;341(6146):673–677.
19. Goenka R, et al. Cutting edge: dendritic cell-restricted antigen presentation initiates the follicular helper T cell program but cannot complete ultimate effector differentiation. *J Immunol*. 2011;187(3):1091–1095.
20. Choi YS, et al. ICOS receptor instructs T follicular helper cell versus effector cell differentiation via induction of the transcriptional repressor Bcl6. *Immunity*. 2011;34(6):932–946.
21. Poholek AC, et al. In vivo regulation of Bcl6 and T follicular helper cell development. *J Immunol*. 2010;185(1):313–326.
22. Kerfoot SM, et al. Germinal center B cell and T follicular helper cell development initiates in the interfollicular zone. *Immunity*. 2011;34(6):947–960.
23. Matloubian M, et al. Lymphocyte egress from thymus and peripheral lymphoid organs is dependent on S1P receptor 1. *Nature*. 2004;427(6972):355–360.
24. Cyster JG, Schwab SR. Sphingosine-1-phosphate and lymphocyte egress from lymphoid organs. *Annu Rev Immunol*. 2011;30:69–94.
25. Massberg S, et al. Immunosurveillance by hematopoietic progenitor cells trafficking through blood, lymph, and peripheral tissues. *Cell*. 2007;131(5):994–1008.
26. Josefowicz SZ, Lu LF, Rudensky AY. Regulatory T cells: mechanisms of differentiation and function. *Annu Rev Immunol*. 2012;30:531–564.
27. Rosenblum MD, Gratz IK, Paw JS, Lee K, Marshak-Rothstein A, Abbas AK. Response to self antigen imprints regulatory memory in tissues. *Nature*. 2011;480(7378):538–542.
28. Bettelli E, et al. Reciprocal developmental pathways for the generation of pathogenic effector TH17 and regulatory T cells. *Nature*. 2006;441(7090):235–238.